The nonlinear Shannon limit and the need for new fibres

A.D.Ellis, N. MacSuibhne, R. Watts, S. Sygletos, F.C.G.Gunning, D.Rafique, J.Zhao

1. INTRODUCTION

Since the first commercial wire-line communication system (telegraph) was deployed by Wheatstone and Cooke in 1839 [1], it may be argued that communications capacity offered to residential customers has increased exponentially at a constant compound annual growth rate of nearly 40% per annum. Today, growth is quantified in terms of the overall internet capacity, where similar overall growth rates are found [2] and is fuelled by a succession of communications applications, each of which evolves through stages of early adoption, increasing penetration and establishment. This was readily seen to be the case of direct dialled telephony, fax and dial up modems, despite transport over a common platform. Similarly, text messaging, image sharing, file sharing and video services represent different applications, sharing a common platform widely referred to as the internet. Recent growth, since the introduction of one of the 1st internet like service, the bulletin board service [3], accessed by dial up modems, through to passive optical networks, still the subject of current research [4] is shown in Figure 1. This figure also illustrates the typical capacity switched within the core, for example today's WDM systems have a total capacity of up to 8 Tbit/s, but typically a single wavelength may be routed using a reconfigurable optical add drop multiplexer and would have a capacity of between 10 and 100 Gbit/s.

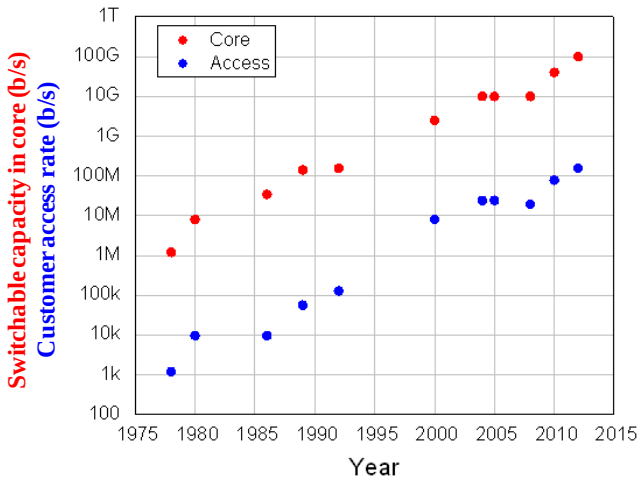

Figure 1: Evolution of access capacity and core network switching granularity since the introduction of BBS.

It is interesting to note that the ratio between the switchable capacity in the core of the network to the access rate has remained close to 1000 over this entire period, despite numerous generations of routing platforms including schemes as diverse as the Plesiochronous Digital Hierarchy (SDH) and Internet Protocol transported by Wavelength Division Multiplexing (IP over WDM). This consistent ratio represents an engineering trade-off between the impact of failures, which favours many separate links, and cost, which favours fewer higher capacity links. Both straw polls of consumer demand and government strategy suggest that the demand for increased consumer bandwidth will be maintained for the foreseeable future as testified by the increasing deployment of optical fibre in the local loop and the design bandwidths of successive generations of wireless technologies. This suggests that we will require the ability to switch capacities of several Tbit/s in the core network, with maximum capacities a few orders of magnitude higher than this. Figure 2 illustrates a common figure of merit for optical communication system experiments, the "bit rate distance product", which combines the two important features: the total bit rate and the maximum transmission distance in a single figure of merit, along with the actual total fibre capacity. Rapid progress was observed throughout the 1980s and 1990s where the decline in growth was observed. This decline was readily attributed to the end of the so called "dotcom boom", which saw a considerable over-deployment of network capacity, in particular of 10 Gbit/s WDM systems. However, once the capacity demand, which continued uninterrupted throughout the crisis, had exhausted this overbuild, whilst total fibre capacities resumed their former growth rate, maximum transmission distances declined, and only a marginal increase in the maximum bit rate distance product is observed, which may be attributed to the adoption of super channels [5] and coherent detection [6] (green symbols). This data may also be analysed as the maximum achievable transmission distance as function of the data rate per wavelength, as shown in Figure 3. From this figure, we can also clearly see that we have exhausted the available transmission capacity of standard single mode fibres. With ingenuity and accommodation of nonlinear effects, it will of course be possible for an ITU grid based system to exceed the theoretical line for standard single mode fibre [7] to a certain extent [8]. However, due to an increase in optical signal-to-noise ratio (OSNR) requirements for multi-level formats, it is clear that, in the region of 1000 Gbit/s, the only

solution is to abandon either the ITU grid or the fibre itself. Until recently, multicarrier modulation was almost exclusively studied to achieve these bit rates, as orthogonal sub-carrier schemes can maximise the capacity of an optical fibre. These schemes were first studied in the 1950s [9] and have been widely used for communication systems susceptible to multi-path degradations, such as wireless, non-coaxial wire-line and multi-mode fibre systems. The technique was introduced into long-haul single mode fibre systems in 2002 [10], and from 2005 a series of publications by a number of groups [11, 12, 13] stimulated worldwide interest. Progress in multi-carrier systems has been rapid, with reports of transmission at 300 Gbit/s, 600 Gbit/s [14], 1 Tbit/s [15] and beyond [16]. Note that precise pulse shaping is required in order to minimise the multiplexing penalty [17, 18], otherwise additional steps must employed to ensure signal orthogonality.

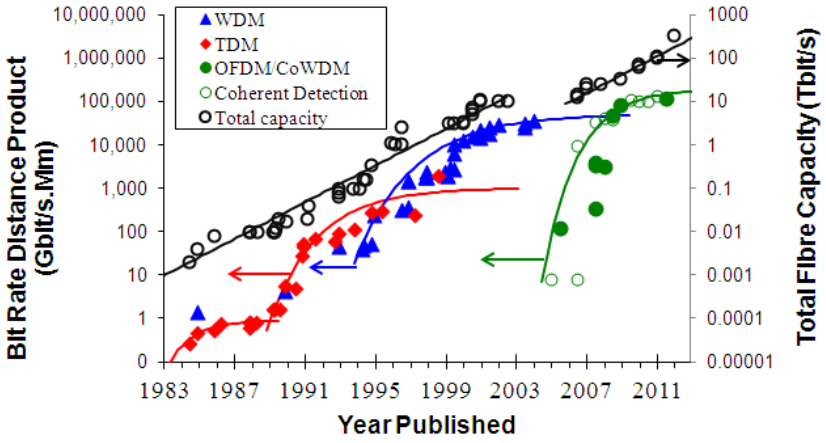

Figure 2: Evolution of the "bit rate distance product" (coloured symbols) and total fibre capacity (black circles) as a function of time showing; time division multiplexing (red diamonds), wavelength division multiplexing (blue triangles), super channels (green circles) and coherent detection (open green circles).

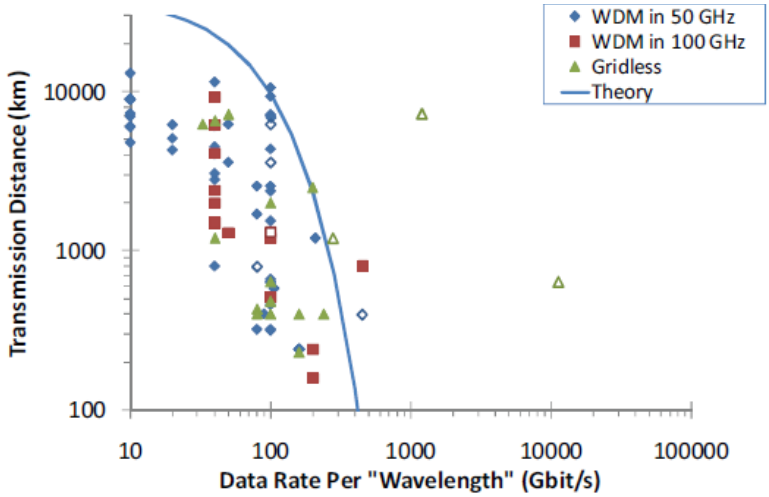

Figure 3 Reach versus data bit rate per transponder (or ROADM routed wavelength) showing the theoretical limit for a symbol rate of 28 Gbaud (blue line) along with experimental results using 50 (blue symbols) and 100 (red symbols) GHz channel spacing, and grid-less experiments (green symbols). Open symbols represent multi-carrier systems, closed symbols single carrier

2. THE NONLINEAR SHANNON LIMIT

The origins of this "capacity crunch", where user demand (Figure 1) appears to be approaching the limits of an optical fibre (Figure 2), is a trade of between the well known Shannon and nonlinearity limits. Shannon predicted that the information capacity of a fixed bandwidth communication channel without memory is proportional to the bandwidth of the channel, and logarithmically proportional to the signal-to-noise ratio. On the other hand, other effects such as chromatic dispersion and nonlinearity induce memory into the channel and induce severe signal distortion. This additional nonlinear distortion limits the maximum power which may be launched into an optical fibre. In the majority of circumstances, the limiting nonlinearity is the optical Kerr effect [19], and accurate predictions may be made using the nonlinear Schrödinger equation, as proposed by Zakharov [20]. Such readily predicted degradations may of course

be compensated by sufficiently sophisticated signal processing [21, 22, 23, 24], and indeed, it has been shown that if the ability to compensate for all nonlinearity in the transmission line is assumed, then the capacity of the communications channel should increase monotonically with signal power [25, 26]. However, if the entire output of the communication channel is not known, either because there is insufficient processing power available [24], or because individual wavelengths propagate along different paths [27], then the unknown signals must be considered as sources of noise to the known signals. This additional noise increases with signal power and prevents the arbitrary increase of the signal-to-noise ratio, and thus imposes a maximum capacity on the communication channel. The existence of this maxima was most famously articulated at the end of the "dotcom" boom [28], and many of the consequences recently summarized in extensive review articles [29, 30]. The original formulation assumes large chromatic dispersion, nonlinearity accumulating over many spans, no nonlinear interaction with noise, and intra channel effects that are either compensated or negligible. The expression derived using this approach is reproduced in equation (1):

$$\frac{C}{B} \cong \log_2(1+snr) = \log_2\left(1+\frac{P_s e^{-\left(\frac{P_S}{P_{NL}}\right)^2}}{P_N + \left(1-e^{-\left(\frac{P_S}{P_{NL}}\right)^2}\right)}\right) \tag{1}$$

where, C is the total capacity of the system occupying a bandwidth B, snr is the signal-to-noise ratio, P_s and P_N the signal and noise power spectral densities respectively, and P_{NL} a "nonlinear power spectral density" scaling factor. For a system with lumped amplifiers the noise and nonlinearity power spectral densities are given by

$$P_N \approx N_a(G-1)n_{sp}.h.\nu \tag{2}$$

$$P_{NL} \approx B\sqrt{\frac{\lambda^2}{c}\frac{B.D.}{\gamma^2 L_{eff}}\frac{\Delta f}{2.\ln\left(N_{ch}/2\right)}} \tag{3}$$

where N_a represents the number of amplified spans, G the amplifier gain, n_{sp} the spontaneous emission noise factor, c the speed of light, h Plank's constant, ν the carrier frequency (λ being the corresponding wavelength), D the chromatic dispersion of the fibre, γ its nonlinear coefficient, and L_{eff} the nonlinear effective length of the overall system (sum of the conventional effective lengths of each span). Δf represents both the channel spacing and the bandwidth of each of the Nch WDM channels. Subsequently, many authors have investigated the problem with a variety of different assumptions, including arbitrary dispersion [31], dominance of four wave mixing [32] and WDM channel bandwidths less than the channel spacing [33]. The majority of these results bear close resemblance to equations (1) to (3), especially if the Taylor series expansion is considered [34] and the predicted capacities agree closely. Detailed numerical simulations [35] reveal that each model performs best for systems with designs matching the assumptions of the model (e.g. OFDM system designs match [32] and Nyquist designs [33]), but even so, except in extreme cases, the trends predicted by the various models are highly correlated. In terms of system configuration, the results are weakly (if at all) dependent on the channel spacing for a large number of channels, and for the fibre parameters, a figure of merit may be derived for a lumped amplifier system;

$$\frac{P_{NL(lumped)}^2}{P_N^2} \propto \left(\frac{1-e^{-\alpha L_{span}}}{\alpha}\right)\left(e^{\alpha L_{span}}-1\right)^2\frac{\gamma^2}{D} \tag{4}$$

where L_{span} represents the span length between amplifiers. This illustrates a weak, but monotonic dependence of absolute value of the dispersion and the nonlinear coefficient. Dependence on fibre loss is more complex due to the trade-off between noise (low loss) and nonlinear effective length (high loss), and care should be taken in generalizing this parameter, and the system configuration (repeater spacing) may have a significant impact on the conclusions [29, 30]. For an ideal Raman amplified system, the situation is clearer, with lower loss always favourable, as shown in equation (5).

$$\frac{P_{NL(idealRaman)}^2}{P_N^2} \propto \frac{\alpha^2 L^3 \gamma^2}{D} \tag{5}$$

with the constants of proportionality readily extracted from equations (2-5). The predictions of these equations may be readily confirmed by numerical simulations [29], and an example of the results which may be achieved is shown in Figure 4, illustrating how the maximum reach reduces for higher order modulation formats.

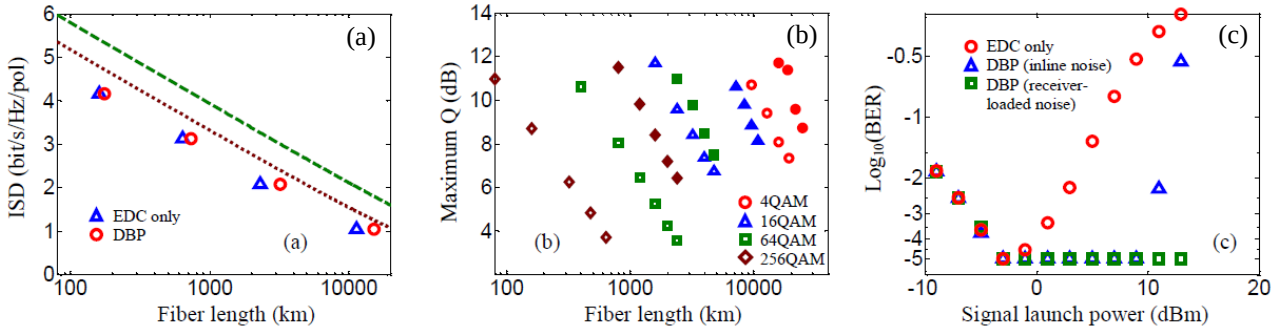

Format	PM-4QAM	PM-16QAM	PM-64QAM	PM-256QAM
Baud rate	28Gbaud	14Gbaud	9.33Gbaud	7Gbaud
Channel spacing	50GHz	25GHz	10GHz	7.5GHz
MUX	30GHz	15GHz	10GHz	7.5GHz
DeMUX	50GHz	25GHz	16.667GHz	12.5GHz
Simulated bits	32,768	65.536	98.304	131.072

Loss (dB/km)	0.2
Dispersion (ps/nm/km)	20
Nonlinearity (1/W/km)	1.5
Length per span (km)	80
Noise Figure (dB)	4.5
Number of channels	9

Figure 4: (a) Theoretical nonlinear capacity limit versus the transmission distance when the in-line dispersion is 20ps/nm/km (dashed line) and 2ps/nm/km (dotted line), and the simulated maximum achievable distance of 4-, 16-, 64-, 256-QAM WDM system for dispersion compensation only (triangles) and single-channel digital back-propagation (DBP), including both dispersion and intra-channel nonlinearity compensation (circles). (b) The maximum achieved Q-factor versus the fiber length by using single-channel back-propagation for DBP in the scenarios of WDM system (open) and single channel (closed). (c) Performance as a function of the signal launch power for a single-channel 112Gbit/s PMQPSK after 4800km with EDC only (circles), DBP with in-line noise loading (triangles) and with receiver-side noise loading (squares). Tables show the simulation parameters used.

In these simulations, there was a penalty in reach of approximately 1dB when compared to the theoretical nonlinear limit with the same dispersion. One reason for this penalty is that the modulation formats and the coding schemes were not optimal. Figure 4 (b) shows the maximum achieved Q-factor at the optimum signal launch power versus the transmission distance for single-channel (closed symbols) and WDM (open symbols) transmission, with both cases using Digital Back-Propagation (DBP) to compensate dispersion and intra-channel nonlinearities. It can be seen that even for the single-channel case where inter-channel nonlinearities are fully compensated, the transmission distance cannot be increased arbitrarily. We may conclude that, for the single channel case, a signal-noise interaction which cannot be compensated by back-propagation must limit the performance, however, the nature of this limitation has, until recently [36], been unknown. To illustrate the cause of this capacity limitation, Figure 4(c) shows the performance of QPSK at a transmission distance of 4,800km versus the signal launch power for the single-channel case, and it is seen that optimal signal launch power exists for not only electronic dispersion compensation (EDC) but also DBP even after intra-channel nonlinearity compensation if noise is loaded along the amplifier chain rather than just at the receiver. In [36], it is shown that this increase in noise with signal power is mainly caused by four-wave mixing between the signal and noise fields, where the simulated amplified noise evolution is consistent with analytical predictions.

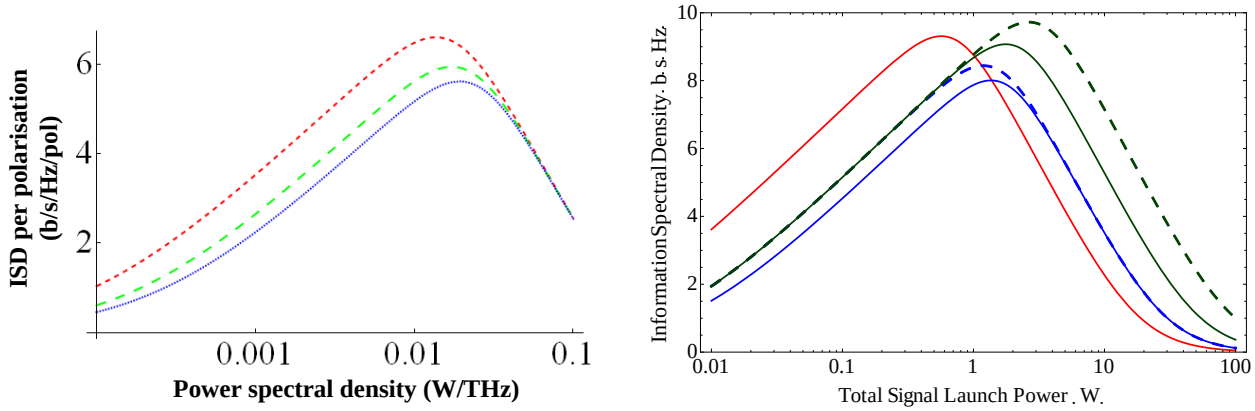

Figure 5 Typical nonlinear Shannon limit curves showing: (left) information spectral density per polarization as a function of the launched power spectral density from each amplifier for noise figures of 4.5 (blue) 3 (green) and 0 (red) dB; and (bottom) the total information spectral density (both polarization) as a function of the total launched power for a fixed information bandwidth for doped fibre amplifiers (blue) with 4.5 (solid) and 3 (dashed) dB noise figures, Raman amplifiers (red) and phase sensitive amplifier with simultaneous idler transmission (green) with 0 (solid) and -3 (dashed) dB noise figures.

Typical plots showing the nonlinear Shannon limit are shown in Figure 5. The left hand chart illustrates the impact of varying the amplifier noise figure alone. This has no effect on the nonlinearity, and so at high powers all three curves

converge. However, in the noise limited region, the same signal-to-noise ratio is obtained at signal launch powers, and, if the noise figure is dropped by 3dB, the signal-to-noise ratio is increased by a factor of two and hence the maximum achievable information spectral density is increased by 1 b/s/Hz/pol. Note that in order to achieve a noise figure below 3dB, it is necessary to use a phase sensitive amplifier where the idlers have also been transmitted along the fibre [37]. In this case, the total signal power (right hand chart in Figure 5) is increased and there is no change in the maximum information spectral density at a fixed total amplifier output power in the signal-to-noise ratio limited regime. On the other hand, in the nonlinear regime, the output power is spread over more channels, reducing the power spectral density, and hence the nonlinear crosstalk between closely spaced channels. However, with both interpretations (signal power spectral density and total amplifier output power) the increase in maximum information spectral density (ISD) due to improvements in amplifier noise figure is small. Similarly, super-channels, either based on OFDM [5, 38] or Nyquist WDM [39], only offer a marginal increase in the ISD due to the elimination of guard bands.

3. OPTICAL REGENERATION

Given that modifications to the transponders and optical amplifiers will have a modest impact on the overall ISD of an optical link, more radical solutions are required. A long standing proposal has been to employ optical regenerators in place of optical amplifiers [40, 41, 42]. However, in order to be cost effective, such regenerators must be WDM compatible and should allow net ISD exceeding that of conventional coherent detection. Whilst WDM compatibility has been demonstrated for a range of modulation formats [42, 43], it is unlikely that the simple binary regenerators demonstrated to date will meet this later criterion. The required regenerator performance may be understood by plotting the nonlinear Shannon limit in terms of the maximum reach between forward error correction modules for a given QAM constellation, as shown in Figure 6.

Given that a PM QPSK system is adequate for the majority of applications, in order to allow the reach to be at least doubled (and at most octupled), the optical regeneration system should be compatible with PM-16QAM data and for formats beyond PM-256QAM, more than 20 regenerators will be required to match the reach of a PM-QPSK digital coherent system. This is a highly challenging target, however recent results are promising, showing black-box WDM [43] and QPSK [44, 45] regeneration and m-PSK processing [46]. Optical regeneration may therefore offer an attractive means to increase fibre capacity, but calculations such as Figure 6 may also be used to estimate an upper bound on the regenerator cost and/or power consumption. For example, comparing M parallel systems employing N_a amplifiers with power consumption P_a to a regenerated system offering M times the maximum capacity per wavelength using N_r regenerators in place of amplifiers, then the power consumption of the regenerator, P_r, should be

$$P_r \le P_a\left((M-1)\frac{N_a}{N_r}+1\right) \tag{5}$$

To illustrate this, consider a 75 span PM-QPSK system (N_a=*75*). To upgrade the capacity by a factor of 4 (M=*4*), we could use four parallel systems, or a single system employing twenty optical regenerators (N_r=*20*) suitable for PM-256QAM. The power consumption of the regenerated system is lower than that of the parallel systems provided that each regenerator consumes less than 12 times the power of the individual optical amplifiers. In the limit of replacing each amplifier by a regenerator (N_a=N_r) , the regenerator power consumption should have less than M times the power consumption of the amplifier to be a power efficient solution.

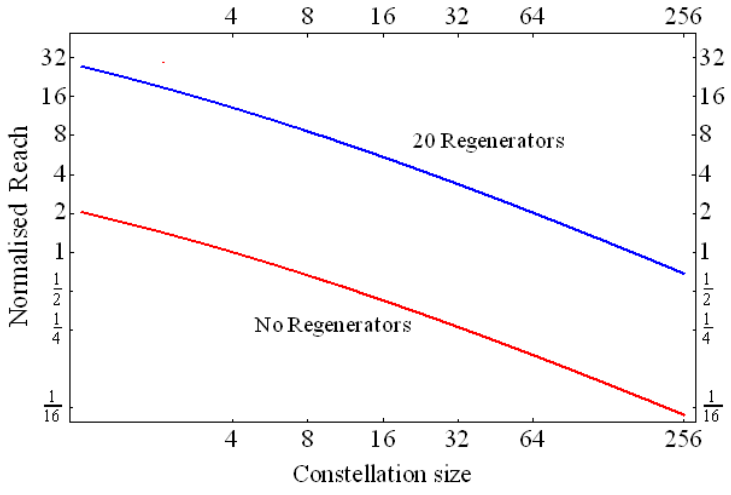

Figure 6 Relative performance limit of digital coherent transmission using optical amplifiers (red) and a system employing 20 optical regenerators (blue) with 80km fibre spans, normalized to the reach of a PM-QPSK system.

4. NOVEL OPTICAL FIBRES

The nonlinear Shannon limit described above gives a fundamental limit on the information spectral density of the fibre, logarithmically directly dependent on the fibre parameters (Equations 1 and 4) and firmly fixed in the region of 5 bit/s/Hz/pol, giving a maximum fibre capacity of the order of 50 Tbit/s in the C-band. Modifications to the amplifier noise figure and modulation format may, in certain circumstances, allow the ISD to be increased by 25-100%, and optical regeneration may enable ISD increases of up to $Log_2(L_{sys}/L_{span})$ per polarization, where L_{sys} is the overall link length, if regenerators ubiquitously replace optical amplifiers (around 8 bit/s/Hz for an ultra long haul system).The capacity limit for conventional single mode fiber is therefore unlikely to increase significantly beyond current levels. However, it is often assumed that the bandwidth demand will continue its uninterrupted 40% compound annual growth experienced since optical systems were first deployed in 1975. Putting 40% growth rates into perspective, if several 100 Gbit/s line cards are installed simultaneously today, to upgrade link capacity in response to demand, similar new deployments in 10 years time would be of fully lit fibres. Widespread cable deployments will be required shortly after this. Since the various techniques to optimise the utilisation of the fibre capacity, including compensation of inter-channel nonlinearity, only offer incremental benefit, major research programs such as EXAT and MODE-GAP are examining novel optical fibres. The fibres may be divided into two broad categories, those enabling spatial multiplexing, such as multi-mode fibres and multi-core fibres, and those aimed at radically reducing the loss and nonlinear coefficients of the fibres.

The baseline solution, of course, is to employ many parallel systems, also known as spatial multiplexing. When employed over conventional fibres, this offers linear power consumption scaling with network capacity whilst demand continues to grow exponentially. For this solution the resultant exponential growth in energy consumption will inevitably result in the imposition of limitations on network capacity through pricing or regulation. But do proposed new fibre types [e.g. 47, 48, 49, 50, 51] offer any substantial benefit in terms of ISD or energy consumption? To gain an initial insight into this question, we may consider an ideal MIMO transmission system, where the nonlinear crosstalk between different modes is entirely neglected. This has previously been justified on the grounds of poor nonlinear phase matching between modes in a few mode fibre. Figure 7 illustrates the minimum pump power summed over all optical amplifiers in the chain required to achieve a given ISD, assuming polarization multiplexing with coherent detection. A challenging 2000km system with 100km spaced fibre amplifiers (no Raman amplification) is chosen as a reference for comparison, and the fibre parameters which have been assumed are summarised in Table 1 and include two types of multi-mode fibre (step index few mode fibre with high differential mode delay, low mode coupling, large effective area but slightly higher loss; and graded index few mode fibre with reduced differential mode delay, and loss and effective areas similar to that of conventional fibre). In Figure 7, each curve is initially signal-to-noise ratio limited and so, as the ISD increases the required power also increases at a fixed rate (see Equation 1). However, once the system is impacted by nonlinearity, the optical signal-to-noise ratio penalty increases the required launch power up to a point where the ISD may no longer be achieved. All four new fibres considered; multi-core fibre (MCF), step index few-mode fibre (SI-FMF), graded index few-mode fibre (GI-FMF) and hollow core photonic band gap fibre (PBGF), offer substantial increases in the achievable ISD, but since the loss of all of the solid core fibres is similar, there is no significant improvement in the signal-to-noise ratio limited performance of each channel, and so no improvement in the required pump power. On the other hand, the theoretically predicted improvements in loss of hollow core PBGF allow for substantial reductions in the required signal launch power, even when the fibre operates with a single mode. Similar conclusions may be drawn for a wide range of system lengths.

Table 1 Fibre parameters used for calculations used unless otherwise specified

Item	**Standard fibre**	**Multi-core fibre**	**Step Index few-mode fibre**	**Graded index few-mode fibre**	**Hollow core fibre**	
System	2000 km					
Repeater	80 km					
Channel	50 GHz					
Dispersion	20 ps/nm/km					
Loss	0.2 dB/km	0.2 dB/km	0.22 dB/km	0.2 dB/km	0.05 dB/km	
Nonlinearity	1.4 /W/km	1.4 /W/km	0.5 /W/km	1.4 /W/km	0.001 /W/km	
Modes	2	2 x 6	6	6	2	6
Wavelength	1550 nm	1550 nm	1550 nm	1550 nm	2000 nm	
Information loss per span	0%	0%	1%	.3%	0%	1%

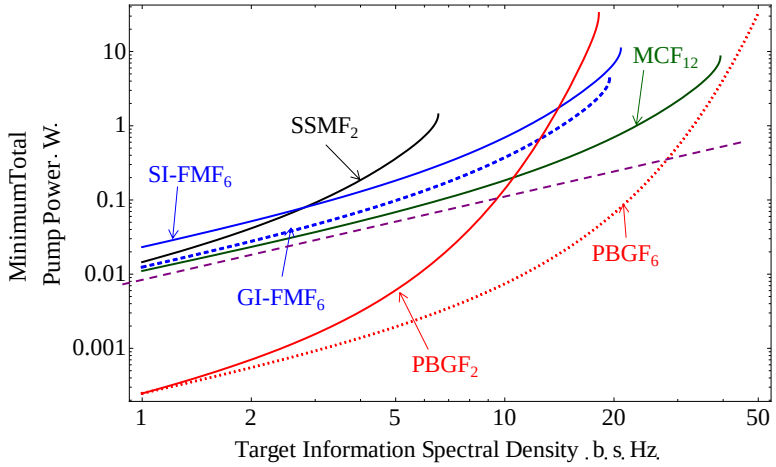

Figure 7: Minimum total pump power (summed over all amplifiers) to achieve a given ISD over a 2000km link with 100km amplifier spacing for conventional fibre (black), graded index few mode fire (blue, dotted), step index few-mode fibre (blue, solid), multi-core fibre (green) and hollow core PCF (red) with (dotted) and without (solid) mode multiplexing. Subscript denotes the total number of modes (including polarizations). The purple line represents a constant pump power per bit.

However, as indicated above, predictions for lumped amplifier systems are critically dependent on the amplifier spacing (Equation 4), and we would anticipate that the relative merits that spatial multiplexing offers and low loss fibre are determined by this parameter. This is illustrated in Figure 8 which shows the required total pump power as a function of the amplifier spacing for a 2000 km system with a target ISD of 10 b/s/Hz. At low repeater spacing, information loss from mode coupling, assumed to be proportional to the number of amplifiers and higher for low differential group delay fibres, imposes a large optical signal-to-noise ratio penalty and dominates the performance of the system. However, for inland networks, where amplifiers are typically spaced 80km apart, the hollow core PBGF offers the lowest required pump power, even when operated as a single mode fibre (two polarisations). If the repeater spacing may be freely selected, for example in a submarine network, spatial multiplexing offers improved performance below 80km, especially using multi-core fibres (or multiple fibres).

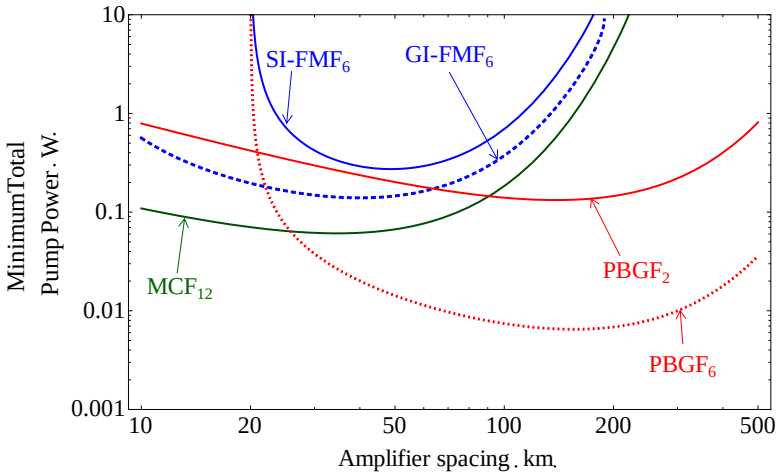

Figure 8 Variation of required total pump power with amplifier spacing for a 2,000km system with an ISD of 10 b/s/Hz. Curves are as specified in Figure 7.

Note that for this system configuration, spatial multiplexing over solid core few-mode fibre offers no significant advantage over multi-core fibres. Again, the conclusion that the energy consumption associated with amplification is minimized by minimizing the fibre loss is true for a wide range of systems lengths and target ISD's. Note also that, in terms of total energy consumption, commercially available fibre amplifiers with output powers in the region of 100mW typically have electrical power consumptions in the region of 10s of Watts [52]. Consequently we may anticipate that the total power consumption of the transmission line would be between 100W and 1kW for a bi-directional system. This should be compared to the power consumption of digital coherent transponders, typically in the region of 1-3 W/Gb [53]. For a 10 Tbit/s system (e.g. 100 channels each at 100 Gbit/s) the transponder power consumption would exceed 10kW, over 10 times the power consumption of the transmission line. Furthermore, one may anticipate that the power consumption associated with the MIMO processing for a few-mode fibre system would be significantly higher than a conventional digital coherent receiver.

The advantage of hollow core PBGF is further emphasised in Figure 9, which takes into account the wide low loss window offered in the 2000nm transmission window predicted for such fibres, and even further enhancements are possible for mode multiplexed operation.

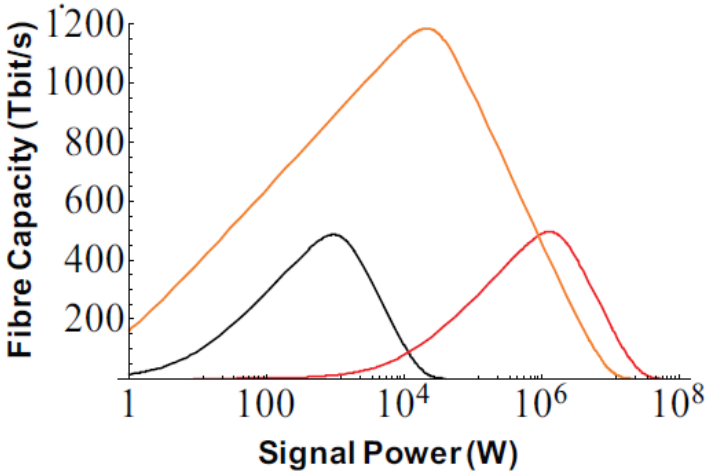

Figure 9: Comparison of the total capacity of a solid core multi-mode fibre with 5-fold mode multiplexing gain (black); a PCF with 0.6 dB/km loss (red), and 0.05 dB/km loss (orange), both operated as single mode fibre. Amplification bandwidth of 100nm for solid core fibre and 600nm for PCF.

5. NONLINEAR PROPAGATION

The above calculations assume negligible nonlinear interaction between the modes, and a minor loss of information due to weak mode dependant loss. However, the first assumption has not been experimentally verified. A simple configuration employing a pulse source, few mode fibre and spectrally resolved detection was employed to perform preliminary investigations into nonlinear propagation [54]. In this case, a 25µm-core diameter fibre supported four LP mode groups, with a maximum differential mode delay (DMD) of 2.95ns/km, chromatic dispersion between 21.1 and 17.5ps/nm/km, and a net loss of less than 10dB including launch splice losses. To avoid pulse collisions due to the modal dispersion within the fibre, an actively mode locked laser (MLL) at 1551nm was used to launch ~23ps pulses at 10MHz repetition rate to the few mode fibre (FMF), with the aid of a 30GHz 3dB bandwidth filter. An EDFA and optical attenuator were used to control the launch power, and the launched pulses were characterized at this point to include any additional distortions from the EDFA. The LP_{01} and LP_{02} modes were excited by making a SMF to FMF fusion splice at both ends, which aligned the claddings of both fibres. This launch, close to centre, ensured that excitement of LP_{11} and LP_21 was negligible. Though this arrangement was effective for exciting only two modes at the input, it also contributed to the high insertion loss and resulted in an uncertainty over the relative input power ratio between the two modes. It is important to note that the input polarization was adjusted at the highest launch power to give the shortest observable pulse width. The output of the FMF was monitored with an oscilloscope via a 50GHz bandwidth photo-detector. In order to recover the phase information, a wavelength selective switch (WSS) was used as a frequency discriminator. The WSS was programmed to give a linear variation in attenuation as a function of frequency, essentially differentiating the temporal field. Comparing information gathered using the 50GHz scope with and without the WSS enabled the amplitude and phase information of the pulse to be extracted. Selected measurements were cross-calibrated using a frequency resolved optical gating (FROG) technique and measurements were found to have good agreement with those that were taken using the frequency discriminator. The results were compared to a numerical model which took into account statistic mode coupling between the excited modes.

At low launch powers, two pulses were observed at the fibre output separated by 56.2ns, in agreement with the calculated DMD taking into account a minimal mode coupling of ~5%. Full field information was recovered for the input signal and for both modes at the output of the 20km length of FMF as a function of the launched signal power. Note that no attempt was made to establish the ratio of launched powers between modes. In order to understand this behaviour, the full width at half-maximum (FWHM) of the output pulses were extracted and plotted in Figure 10 against the relative input powers per mode for each of the excited modes. The experimental measurements of LP_{01} (circles) and LP_{02} (squares) are compared with FMF model simulations (crosses and asterisks respectively), and also with a one step split-step analysis (solid and dashed lines respectively). In this case, the FMF is modelled as SPM followed by dispersion, as it would be in an SMF case with the addition of mode coupling, where bandwidth limitations of the experimental components were considered. Here, the mode coupling gives dips in the output pulse width, and the position and amplitude of the dips are power dependent. Whether this is a result of nonlinear mode coupling or of changes in the signal spectrum (wavelength dependent mode coupling) will be the subject of a future investigation. For LP_{01}, SPM clearly plays a role by narrowing the pulses as the power increases. As the power is increased further (over

10dB), the nonlinearities induce pulse splitting, and the FWHM measurements begin to increase dramatically. Note that the two solid circle symbols correspond to pulse splitting for LP01, and the FWHM shown in these two cases were obtained by measuring the FWHM of the overall pulse by measuring the sum of the two split pulses, considering an even power split.

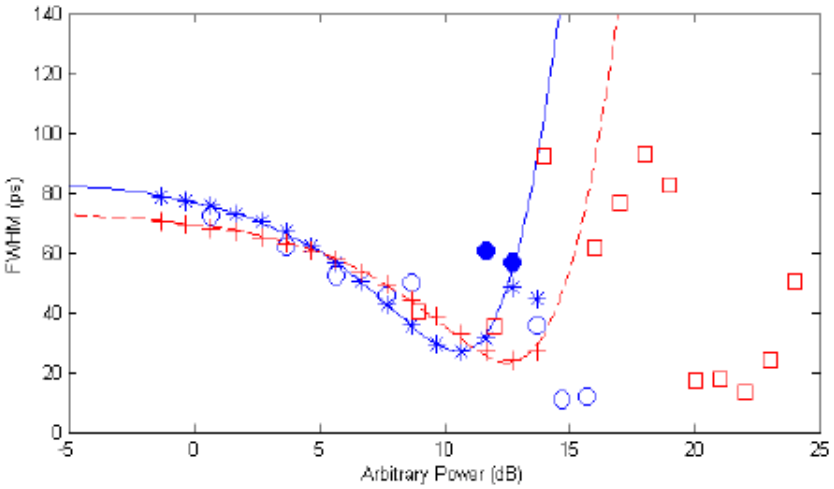

Figure 10 FWHM width measurements for both LP_{01} (circles) and LP_{02} (squares).

We may thus conclude that, at modest launch powers, each mode behaves as if it were propagating along the equivalent single mode fibre. However, at higher launch powers, rapid pulse break up, inconsistent with this simple approximation, is readily observed. Whilst occurring for high peak powers in this simple test, for the highest capacity systems may require similar total launch powers when mode and wavelength division multiplexing are taken into account.

6. CONCLUSIONS

In this document we have considered the implications of the nonlinear Shannon limit, and in particular the consequences for transmission link designs which would meet the growing demand for bandwidth without significant increases in energy consumption. Whilst many techniques are found to offer the potential for capacity increases, the logarithmic nature of the limit implies that even optical regeneration only offers an ISD increase of 2 to 3 times. The techniques will delay a capacity crunch associated with energy consumption. In terms of energy consumption, loss is clearly seen to be the dominant parameter with low loss hollow core PBGF offering the lowest link power consumption for a wide range of system configurations.

7. ACKNOLWLEDGEMENTS

This work has been supported by Science Foundation Ireland under Grant 06/IN/I969, the Irish Higher Education Authority via the INSPIRE programme and by the EU FP7-ICT programme under grant agreements 228033 (MODE-GAP) and 224547 (PHASORS).

8. REFERENCES

[1] The Electromagnetic Telegraph, J. B. Calvert, 19 May 2004 (http://mysite.du.edu/~jcalvert/tel/morse/morse.htm#P).
[2] Cisco white paper (June 2011). Entering the Zettabyte Era, 2010–2015, http://www.cisco.com/en/US/netsol/ns827/networking_solutions_white_papers_list
[3] Collection of Memories of writing and running the first BBS by Ward Christensen (Circa 1992), BBSDocumentary.com, retrieved June 30, 2007 (http://www.bbsdocumentary.com/software/AAA/AAA/CBBS/memories.txt)
[4] P. Ossieur, C. Antony, A. M. Clarke, A. Naughton, H.-G. Krimmel, Y. Chang, C. Ford, A. Borghesani, D. G. Moodie, A. Poustie, R. Wyatt, B. Harmon, I. Lealman, G. Maxwell, D. Rogers, D. W. Smith, D. Nesset, R. P. Davey, P. D. Townsend, "A 135-km 8192-Split Carrier Distributed DWDM-TDMA PON With 2 x 32 x 10 Gb/s Capacity," J. Lightwave Technol. Vol. 29, pp 463-474 (2011).

[5] A.D.Ellis, F.C.G.Gunning, “Spectral Density Enhancement using Coherent WDM”, Photonics Technology Letters, Vol. 17, No. 2, 504-506, (2005)
[6] M. G. Taylor, “Coherent detection method using DSP for demodulation of signal and subsequent equalization of propagation impairments,” IEEE Photon. Technol. Lett., vol. 16, no. 2, pp. 674–676, Feb. 2004
[7] A. D. Ellis, D.Rafique, S.Sygletos, “Capacity in Fiber Optic Communications– The Case for a Radically New Fiber,” IPC 2011, paper TuN1.
[8] D. Rafique and A. D. Ellis, “Impact of signal-ASE four-wave mixing on the effectiveness of digital back-propagation in 112 Gb/s PM-QPSK systems”, Optics Express, Vol. 19, No. 4, pp. 3449, (2011)
[9] R.R. Mosier, R.G. Clabaugh, “Kineplex, a bandwidth-efficient binary transmission system”, AIEE Trans., Vol. 76, pp. 723-728 (1958)
[10] H. Sanjoh, E. Yamada, and Y. Yoshikuni, “Optical orthogonal frequency division multiplexing using frequency/time domain filtering for high spectral efficiency up to 1 bit/s/Hz”, OFC 2002, paper ThD1 (2002)
[11] A.D.Ellis, F.C.G.Gunning, “Achievement of 1 bit/s/Hz Information Spectral Density Using Coherent WDM”, OFC 2005, Paper OThR4, (2005).
[12] A.J. Lowery, L. Du, and J. Armstrong, “Orthogonal frequency division multiplexing for adaptive dispersion compensation in long haul WDM systems”, OFC 2006, PDP39 (2006).
[13] I.B. Djordjevic, B. Vasic, “Orthogonal frequency division multiplexing for high-speed optical transmission”, Opt. Express, vol.14, no.9, pp. 3767–3775 (2006).
[14] F.C. Garcia Gunning. T. Healy, X. Yang, A.D. Ellis, “0.6Tbit/s Capacity and 2bit/s/Hz Spectral Efficiency at 42.6Gsymbol/s Using a Single DFB Laser with NRZ Coherent WDM and Polarisation Multiplexing”, CLEO Europe 2007, paper CI8-5, (2007).
[15] Y.Ma, Q.Yang, Y.Tang, S.Chen, and W.Shieh , “1-Tb/s per channel coherent optical OFDM transmission with subwavelength bandwidth access”, OFC 2009, PDPC1 (2009)
[16] D. Hillerkuss, R. Schmogrow, T. Schellinger, M. Jordan, M. Winter, G. Huber, T. Vallaitis, R. Bonk, P. Kleinow, F. Frey, M. Roeger, S. Koenig, A. Ludwig, A. Marculescu, J. Li, M. Hoh, M. Dreschmann, J. Meyer, S. Ben Ezra, N. Narkiss, B. Nebendahl, F. Parmigiani, P. Petropoulos, B. Resan, A. Oehler, K. Weingarten, T. Ellermeyer, J. Lutz, M. Moeller, M. Huebner, J. Becker, C. Koos, W. Freude & J. Leuthold, “26 Tbit s-1 line-rate super-channel transmission utilizing all-optical fast Fourier transform processing” Nature Photonics, Vol. 5,, pp 364–371, (2011)
[17] G. Bosco, V. Curri, A. Carena, P. Poggiolini, and F. Forghieri. “On the Performance of Nyquist-WDM Terabit Superchannels Based on PM-BPSK, PM-QPSK, PM-8QAM or PM-16QAM Subcarriers”, JLT Vol.29, No. 1, pp. 53-61 (2011).
[18] J. Zhao and A. D. Ellis, “Electronic Impairment Mitigation in Optically Multiplexed Multicarrier Systems”, Journal of Lightwave Technology, Vol. 29, No. 3, pp278, (2011).
[19] R. Y. Chiao, E. Garmire, and C. H. Townes , “Self-trapping of optical beams”, Phys. Rev. Lett. Vol. 13, No. 15, pp479-482 (1964).
[20] A. Hasegawa and F. Tappert, “Transmission of stationary nonlinear optical pulses in dispersive dielectric fibers I. Anomalous dispersion”, Appl. Phys. Lett., vol. 23, pp. 142–144, 1973.
[21] S. Watanabe, S. Kaneko, T. Chikama, “Long-HaulFiberTransmission Using OpticalPhaseConjugation”, Optical Fiber Technology, Vol. 2, No. 2, pp 169–178 (1996)
[22] M. Nakazawa,E. Yamada, H. Kubota, K. Suzuki , "10 Gbit/s soliton data transmission over one million kilometres," Electronics Letters , vol.27, no.14, pp.1270-1272, (1991).
[23] G. Goldfarb, M.G. Taylor, G. Li; , "Experimental demonstration of fiber impairment compensation using the split-step infinite impulse response method", Digest of the IEEE/LEOS Summer Topical Meetings 2008, pp.145-146, (2008).
[24] D. Rafique, J. Zhao, and A. D. Ellis, "Digital back-propagation for spectrally efficient WDM 112 Gbit/s PM m-ary QAM transmission," Opt. Express 19, 5219-5224 (2011)
[25] K. S. Turitsyn, S. A. Derevyanko, I. V. Yurkevich and S. K. Turitsyn, Information capacity of optical fiber channels with zero average dispersion, Phys. Rev. Lett. 91 203091 (2003).
[26] E. Agrell, “The channel capacity increases with power”, preprint arXiv:1108.0391v2 (2012).
[27] T. Freckmann, R.-J. Essiambre, P.J. Winzer, G.J. Foschini, G. Kramer, "Fiber Capacity Limits With Optimized Ring Constellations," Photonics Technology Letters, IEEE , vol.21, no.20, pp.1496-1498, (2009).
[28] P. P. Mitra and J. B. Stark "Nonlinear limits to the information capacity of optical fibre communications", Nature, vol. 411, pp.1027, (2001).
[29] R.-J. Essiambre, G. Kramer, P.J. Winzer, G.J. Foschini, B. Goebel, “Capacity limit of optical fiber networks”, IEEE Journal of Lightwave Technology, vol. 28, no.4, pp662-701, (2010)
[30] A.D.Ellis, J. Zhao, D. Cotter, “Approaching the Non-linear Shannon Limit”, Journal of Lightwave Technology, Vol. 28, No. 4, pp 423 – 433, (2010).
[31] J. Tang, “A comparison study of the Shannon channel capacity of various nonlinear optical fibers”, Journal of Lightwave technology, 24, No. 5, pp. 2070-2075 (2006)
[32] X. Chen, and W. Shieh, “Closed-form expressions for nonlinear transmission performance of densely spaced coherent optical OFDM systems,” Opt. Express 18(18), 19039–19054 (2010).

[33] P.Poggiolini, A. Carena, V. Curri, G. Bosco, F. Forghieri, "Analytical Modeling of Nonlinear Propagation in Uncompensated Optical Transmission Links," Photonics Technology Letters, IEEE , vol.23, no.11, pp.742-744, (2011)
[34] A.D.Ellis, D.Rafique, S.Sygletos, "Capacity in Fibre Optic Communications: The Case for a Radically New Fibre", IEEE Photonics Conference 2011, paper TuN1 (2011).
[35] S. Kilmurray, T. Fehenberger, P. Bayvel, and R. I. Killey, "Comparison of the nonlinear transmission performance of quasi-Nyquist WDM and reduced guard interval OFDM," Opt. Express 20, 4198-4205 (2012).
[36] D. Rafique et al, OFC'11, paper OThO2
[37] Z. Tong, C. Lundström, P. A. Andrekson, C. J. McKinstrie, M. Karlsson, D. J. Blessing, E. Tipsuwannakul, B. J. Puttnam, H. Toda & L. Grüner-Nielsen, "Towards ultrasensitive optical links enabled by low-noise phase-sensitive amplifiers", Nature Photonics, Vol. 5, pp430–436, (2011).
[38] D. Hillerkuss, R. Schmogrow, T. Schellinger, M. Jordan, M. Winter, G. Huber, T. Vallaitis, R. Bonk, P. Kleinow, F. Frey, M. Roeger, S. Koenig, A. Ludwig, A. Marculescu, J. Li, M. Hoh, M. Dreschmann, J. Meyer, S. Ben Ezra, N. Narkiss, B. Nebendahl, F. Parmigiani, P. Petropoulos, B. Resan, A. Oehler, K. Weingarten, T. Ellermeyer, J. Lutz, M. Moeller, M. Huebner, J. Becker, C. Koos, W. Freude, J. Leuthold, "26 Tbit/s line-rate super-channel transmission utilizing all-optical fast Fourier transform processing", Nature Photonics, Vol. 5, pp364–371, (2011)
[39] G. Bosco, V. Curri, A. Carena, P. Poggiolini, and F. Forghieri, "On the Performance of Nyquist-WDM Terabit Superchannels Based on PM-BPSK, PM-QPSK, PM-8QAM or PM-16QAM Subcarriers," J. Lightwave Technol. 29, 53-61 (2011)
[40] W.A.Pender, T.Widdowson, A.D.Ellis, "Error free operation of a 40 Gbit/s all optical regenerator", Elect Lett, Vol.32, No.6, pp 567, (1996)
[41] D. Cotter, R.J.Manning, K.J.Blow, A.D.Ellis, A.E.Kelly, D.Nesset, I.D.Phillips, A.J.Poustie, D.C.Roger , "Nonlinear Optics for High-Speed Digital Information Processing", Science, Vol. 286, No5444, pp1523-, (1999)
[42] O. .Leclerc et al., "All-Optical Regeneration: Key Features and Application to a 160Gbit/s (4x40Gbit/s) Long-Haul Transmission", IEEE LEOS newsletter, Vol. 14, No.4, (2000).
[43] S. Sygletos, P. Frascella, S.K. Ibrahim, L. Grüner-Nielsen, R. Phelan, J. O'Gorman, A.D. Ellis "A Practical Phase Sensitive Amplification Scheme for Two Channel Phase Regeneration", Optics Express Vol. 19, Iss. 26, pp. B938–B945 (2011).
[44] R. Slavík, F. Parmigiani, J. Kakande, C. Lundström , M. Sjödin, P. A. Andrekson, R. Weerasuriya, S. Sygletos, A. D. Ellis, L. Grüner-Nielsen, D. Jakobsen, S.. Herstrøm, R. Phelan, J. O'Gorman, A. Bogris, D. Syvridis, S. Dasgupta, P. Petropoulos, D. J. Richardson, "All-optical phase and amplitude regenerator for next-generation telecommunications systems", Nature Photonics Vol. 4, No. 10, pp690-695 (2010).
[45] R. P. Webb, J. M. Dailey, R. J. Manning, and A. D. Ellis, "Phase discrimination and simultaneous frequency conversion of the orthogonal components of an optical signal by four-wave mixing in an SOA," Optics Express 19, 20015-20022 (2011).
[46] J.Kakande, R.Slavík, F. Parmigiani, A. Bogris, D. Syvridis, L. Grüner-Nielsen, R. Phelan, P. Petropoulos, D. J. Richardson, "Multilevel quantization of optical phase in a novel coherent parametric mixer architecture", Nature Photonics, Vol. 5,Pages:748–752, (2011) .
[47] H. Takara, H. Ono, Y. Abe, H. Masuda, K. Takenaga, S. Matsuo, H. Kubota, K. Shibahara, T. Kobayashi, and Y. Miaymoto, "1000-km 7-core fiber transmission of 10 x 96-Gb/s PDM-16QAM using Raman amplification with 6.5 W per fiber," Opt. Express 20, 10100-10105 (2012)
[48] P. Sillard, M. Astruc, D. Boivin, H. Maerten, and L. Provost , "Few-Mode Fiber for Uncoupled Mode-Division Multiplexing Transmissions," Proceedings of ECOC, paper Tu.5.LeCervin.7 (2011)
[49] L. Grüner-Nielsen, Y. Sun, J. W. Nicholson, D. Jakobsen, R. Lingle Jr, and B. Pálsdóttir, "Few Mode Transmission Fiber with low DGD, low Mode Coupling and low Loss", Proc OFC 2012, paper PDP5A1 (2012)
[50] K. Imamura, H. Inaba, K. Mukasa, and R. Sugizaki, "Weakly Coupled Multi Core Fibers with Optimum Design to Realize Selectively Excitation of Individual Super-modes," in Optical Fiber Communication Conference, OSA Technical Digest (Optical Society of America, 2012), paper OM2D.6. (2012)
[51] N. V. Wheeler, M. N. Petrovich, R. Slavik, N. K. Baddela, E. R. Numkam Fokoua, J. R. Hayes, D. Gray, F. Poletti, and D. Richardson, "Wide-bandwidth, low-loss, 19-cell hollow core photonic band gap fiber and its potential for low latency data transmission," in National Fiber Optic Engineers Conference, OSA Technical Digest (Optical Society of America, 2012), paper PDP5A.2 (2012)
[52] W. Van Heddeghem, F. Idzikowski, W. Vereecken, D. Colle, M. Pickavet, and P. Demeester, "Power consumption modeling in optical multilayer networks", Photonic Network Communications (2012),
[53] A. Morea, S. Spadaro, O. Rival, J. Perelló, F. Agraz and D. Verchere, "Power Management of Optoelectronic Interfaces for Dynamic Optical Networks", ECOC 2011, paper , (2011)
[54] N. Mac Suibhne, R. Watts, S. Sygletos, F.C Garcia Gunning, L. Grüner-Nielsen, and A.D. Ellis, "Nonlinear Pulse Distortion in Few-Mode Fiber", ECOC 2012, paper Th.2.F.5 (2012)